Biochemical Engineering Journal 41 (2008) 95–103

Contents lists available at ScienceDirect

Biochemical Engineering Journal

journal homepage: www.elsevier.com/locate/bej

Kinetic modelling of aldolase-catalyzed addition between dihydroxyacetone phosphate and (*S*)-alaninal

Trinitat Suau, Gregorio Álvaro, M. Dolors Benaiges, Josep López-Santín*

Departament d'Enginyeria Química, Escola Tècnica Superior d'Enginyeria, Unitat de Biocatàlisi Aplicada associada al IIQA (CSIC), Universitat Autònoma de Barcelona, Campus de Bellaterra, Edifici Q, 08193 Bellaterra, Spain

ARTICLE INFO

Article history:
Received 29 November 2007
Received in revised form 15 February 2008
Accepted 2 April 2008

Keywords:
Aldolases
Kinetic model
Stereoselective synthesis
Fuculose-1-phosphate aldolase

ABSTRACT

This paper is focused on the development of a kinetic model for an aldolase-catalyzed reaction. The aldol addition between dihydroxyacetone phosphate (DHAP) and (*S*)-benzyloxycarbonyl-alaninal ((*S*)-Cbz-alaninal) catalyzed by the four DHAP-dependent aldolases is a promising way for the synthesis of four complementary diastereoisomers with potential biological activity. The reaction catalyzed by fuculose-1-phosphate aldolase (FucA) conducts to a synthesis product with a 100% diastereomeric excess. A kinetic model has been proposed including both the synthesis and a parallel non-desired secondary reaction. The model involved an ordered two-substrate mechanism for the synthesis and non-competitive inhibition by (*S*)-Cbz-alaninal and competitive inhibition by methylglyoxal byproduct in both reactions. The values of the model kinetic parameters were determined and the model validated in batch and fed-batch synthesis reactions. The obtained model could be extended to explain the behavior of other class II DHAP-dependent aldolases and exploited in simulation for reactor design purposes.

1. Introduction

Aldolases are biocatalysts of great interest in chiral synthetic processes because they are able to catalyze C–C bond formation controlling the regio and stereospecifity of aldol addition reactions [1–4]. The synthetic abilities of aldolases have been emphasized in a great number of reports and reviews in the recent literature [2,5]. Most of the synthetic papers are mainly focused in the exploitation of the stereoselectivity of these enzymes in the formation of C–C bonds [1,6–8].

The four enzymes of the family of dihydroxyacetone phosphate (DHAP)-dependent aldolases, fructose-1,6-bisphosphate aldolase (FruA, EC 4.1.2.13), fuculose-1-phosphate aldolase (FucA, EC 4.1.2.17), rhamnulose-1-phosphate aldolase (RhuA, EC 4.1.2.19) and tagatose-1,6-bisphosphate aldolase (TagA, EC 4.1.2.40), catalyze *in vivo* the reversible asymmetric addition of DHAP to D-glyceraldehyde 3-phosphate (G3P) or L-lactaldehyde. These enzymes have been proven to be useful in synthesis because they catalyze the aldol addition of DHAP with a wide range of acceptor aldehydes conducting to products with two new stereogenic centers. Depending of the employed enzyme, α, β-dihydroxyketones of complementary stereochemistry can be obtained [8,9]. For class II DHAP-dependent aldolases, the catalytic mechanism has been elucidated at molecular level [10,11] and studies on the suitable acceptor aldehydes in the synthesis of valuable products have been reported with a focus on organic synthesis [2,6,8]. Nevertheless, there is a lack of papers concerning kinetic models and kinetic data. This is necessary information in order to design appropriate reactors and to improve the performance of aldolase-catalyzed synthetic processes.

Iminocyclitols are inhibitors of glycosidases and glycosyltransferases, with a great therapeutic potential for a wide range of diseases. The key synthetic step is the DHAP-dependent aldolase-catalyzed aldol addition of DHAP to Cbz-aminoaldehydes to render aminopolyols, precursors of iminocyclitols [12–14]. In particular, the aldol addition between DHAP and (*S*)-Cbz-alaninal by the four DHAP-dependent aldolases has been proposed as a promising way for the synthesis of four complementary diastereoisomers with potential biological activity.

In previous work [15], the significance of chemical and enzymatic DHAP degradation in class II aldolase-catalyzed syntheses has been reported, employing the above mentioned synthesis catalyzed by FucA. Published results using recombinant His-tagged FucA produced in our laboratory, led to the synthesis product with a 100% diastereomeric excess [16].

The objective of the present paper is to develop a kinetic model for the target aldolase-catalyzed reaction, and to validate its usefulness in reactor design by properly describing both batch and fed-batch reaction processes.

* Corresponding author. Tel.: +34 935811806; fax: +34 935812013.
E-mail address: Josep.lopez@uab.cat (J. López-Santín).

1369-703X/$ – see front matter © 2008 Elsevier B.V. All rights reserved.
doi:10.1016/j.bej.2008.04.002

2. Materials and methods

2.1. Materials

Dihydroxyacetone phosphate dilithium salt ($DHAPLi_2$) was purchased from Fluka.

(*S*)-Cbz-alaninal was synthesized in our laboratory by 2-iodobenzoic acid oxidation of the corresponding N-protected amino alcohol as reported in literature [14,15,17].

Fuculose-1-phosphate was synthesized as dicyclohexylamine salt according to reported procedures [15,18,19].

Recombinant FucA was expressed in *E. coli* strain XL1 blue MRF' (pTrcfuc) and produced in a 2L BiostatB (Braun Biotech Int.) fermentor in fed-batch mode [20]. Cells were disrupted by ultrasonication and the intracellular aldolase was purified by metal-chelate affinity chromatography and $(NH_4)_2SO_4$ precipitation after $ZnSO_4$ incubation. The final preparation had an average specific activity of 10 activity units (AU)/mg and was stored at 4 °C [15].

All other chemicals were of analytical grade.

2.2. Experimental procedures

2.2.1. Enzymatic aldol additions

The synthesis reactions used for model calibration were carried out in dimethylformamide (DMF)/water (20%, v/v) at the initial substrate concentrations shown in Table 2. The aldehyde (*S*)-Cbz-alaninal was dissolved in 1 mL of DMF and added to $DHAPLi_2$ dissolved in 4 mL aqueous buffer solution to get a final concentration of 50 mM Tris–HCl, 150 mM KCl at pH 7.0. Then, to start the reaction, FucA aldolase was added to get an enzyme concentration of 3 AU/mL, and the reaction medium was maintained under constant stirring at 4 °C.

The two reactions employed for model validation experiments were performed at 12 AU/mL. The batch reaction was carried out at 27.8 mM DHAP and 43 mM aldehyde initial concentration. The reaction with discrete DHAP additions was prepared as mentioned above with exception of DHAP which was added in 5 additions of 0.027 mmol each (0.135 mmol total amount) and at an initial concentration of (*S*)-Cbz-alaninal of 46 mM.

The progress of the reactions was followed by measuring DHAP, (*S*)-Cbz-alaninal and aldol adduct concentration by the analytical methods depicted below.

2.2.2. Secondary reaction of DHAP consumption

The enzyme-catalyzed DHAP disappearance in absence of aldehyde was performed in DMF/water (20%, v/v) at 4 °C. A reaction volume of 2.5 mL at different initial DHAP concentrations (27.5, 47.0, 136, 216, 297, 445 mM), was prepared by addition of 0.5 mL of DMF and 2 mL of a $DHAPLi_2$ aqueous solution in order to obtain a final concentration of 50 mM Tris–HCl 150 mM KCl at pH 7.0.

2.2.3. Inhibition studies

2.2.3.1. Phosphate inhibition. The reactions were performed at 4 °C in a volume of 2.5 mL at 40 mM initial concentration of DHAP and different initial amounts of sodium phosphate 13, 33, 70, 109, 174 and 268 mM. Reaction medium was prepared by addition of 0.5 mL of DMF and a $DHAPLi_2$ aqueous solution in order to obtain the desired final concentration of sodium phosphate and 150 mM KCl at pH 7.0. FucA aldolase was added to get an enzyme concentration of 3 AU/mL and the evolution of DHAP concentration with time was measured.

2.2.3.2. Methylglyoxal inhibition. The reactions were performed at 4 °C in a volume of 2.5 mL at 40 mM initial concentration of DHAP and different initial amounts of methylglyoxal 50, 120 and 200 mM. Reaction medium was prepared by addition of 0.5 mL of DMF and a $DHAPLi_2$ aqueous solution in order to obtain the desired final concentration of methylglyoxal and 50 mM Tris–HCl 150 mM KCl at pH 7.0. FucA aldolase was added to get an enzyme concentration of 3 AU/mL and the evolution of DHAP concentration with time was measured.

2.2.3.3. (S)-Cbz-alaninal inhibition. A reaction volume of 5 mL at 12 mM initial DHAP concentration and different initial (*S*)-Cbz-alaninal concentrations (14.5, 27.7, 34.9, 41.4, 60.3, 70.5 mM), was prepared at 4 °C by addition of (*S*)-Cbz-alaninal dissolved in 1 mL of DMF and a $DHAPLi_2$ aqueous solution in order to obtain a final concentration of 50 mM Tris–HCl 150 mM KCl at pH 7.0. FucA aldolase was added to get an enzyme concentration of 3 AU/mL and the evolution of DHAP concentration with time was measured.

2.3. Analytical methods

2.3.1. FucA activity assay

FucA activity was measured using a coupled enzymatic assay. In the first step, fuculose-1-phosphate is cleaved to L-lactaldehyde and DHAP by FucA; in the second step, DHAP is reduced using rabbit muscle glycerol 3-phosphate dehydrogenase (GDH) and reduced nicotine adenine dinucleotide (NADH). The following reactants were mixed in a 1 mL cuvette and maintained at 25 °C: 34 μL of fuculose-1-phosphate 58 mM, 34 μL of NADH 4 mM, 34 μL of GDH 50 AU/mL and 864 μL of 100 mM Tris–HCl buffer 150 mM KCl pH 7.5 at 25 °C. The assay was initiated upon addition of 34 μL of the sample to be titrated for aldolase activity. One activity unit (AU) of FucA is defined as the amount of enzyme that catalyzes the hydrolysis of 1 μmol of fuculose-1-phosphate to DHAP and L-lactaldehyde per minute at 25 °C and pH 7.5. The time course of the reaction was followed measuring the decrease of NADH by monitoring the absorbance at 340 nm in a UV–vis Cary (Varian) spectrophotometer ($\varepsilon = 6.22\ mM^{-1}\ cm^{-1}$). The linear range of the assay is between 0.19 and 0.60 AU [20].

2.3.2. Assay of dihydroxyacetone phosphate

Dihydroxyacetone phosphate concentration was determined spectrophotometrically. DHAP is reduced using rabbit muscle GDH and NADH. The following reactants were mixed in a 1 mL cuvette and maintained at 25 °C: 10 μL of 20 mM NADH, 10 μL of DHAP sample and 970 μL of 100 mM Tris–HCl buffer pH 7.5. The assay was initiated upon addition of 10 μL of GDH (50 U/mL). The time course of the reaction was followed measuring the decrease of NADH absorbance at 340 nm before (Abs_1) and after (Abs_2) GDH addition in a UV–vis Cary (Varian) spectrophotometer ($\varepsilon = 6.22\ mM^{-1}\ cm^{-1}$). The DHAP concentration can be obtained using the equation $[DHAP]\ (mM) = (Abs_1 - Abs_2)/(6.22\ mM) \times 100$. The linear range of the assay is until 15 mM of DHAP.

2.3.3. Analysis of (S)-Cbz-alaninal and synthesis product by HPLC

HPLC analyses were performed on a HPLC system (Waters™ LC Module I plus) fitted with RP-HPLC cartridge, 250 mm × 4 mm filled with Lichrosphere® 100, RP-18, 5 μm (Merck). The solvent system was the following: solvent A: 0.1% (v/v) trifluoroacetic acid (TFA) in H_2O, solvent B: 0.095% (v/v) TFA in H_2O:CH_3CN 1:4 (v/v); gradient elution from 10 to 70% B in 30 min, flow rate 1 mL min^{-1}, UV detection at 215 nm. Samples (20 μL) were withdrawn from the reaction medium, dissolved with methanol (380 μL), and analyzed subsequently by HPLC. Quantitative analysis of (*S*)-Cbz-alaninal and product was performed from peak areas by the external standard method.

2.4. Model parameters estimation using gPROMS

gPROMS software (PROcess Modelling System) for simulation, optimization and parameter estimation of highly complex processes was utilized. Parameter estimation attempts to determine values for the unknown parameters, θ, in order to maximize the probability that the mathematical model will predict the values obtained from the experiments. Assuming independent, normally distributed measurement errors, ε_{ijk}, with zero means and standard deviations, σ_{ijk}, this maximum likelihood goal can be captured through the following objective function:

$$\phi = \frac{N}{2}\ln(2\pi) + \frac{1}{2}\min_{\theta}\left\{\sum_{i=1}^{NE}\sum_{j=1}^{NV_i}\sum_{k=1}^{NM_{ij}}\left[\ln(\sigma_{ijk}^2) + \frac{(\tilde{z}_{ijk} - z_{ijk})^2}{\sigma_{ijk}^2}\right]\right\}$$

where Φ, objective function; N, total number of measurements taken during all the experiments; θ, set of model parameters to be estimated; NE, number of experiments performed; NV_i, number of measured variables in the ith experiment; NM_{ij}, number of measurements of the jth variable in the ith experiment; σ_{ijk}^2, variance of the kth measurement of variable j in experiment i; z_{ijk}, kth measured value of variable j in experiment I; z_{ijk}, kth (model-) predicted value of variable j in experiment i.

3. Results and discussion

3.1. Model development

For class II aldolases, as is the case of the recombinant FucA employed, there are three parallel reactions to be considered: (a) aldol addition between DHAP and (*S*)-Cbz-alaninal; (b) DHAP enzymatic degradation; (c) DHAP chemical degradation. It has been demonstrated that both the desired and non-desired enzymatic reactions take place through the same enediolate intermediate [15].

As the main objective is the aminopolyol production, the process has been performed under previously selected optimal operational conditions. The aldolase-catalyzed syntheses took place at 4 °C in DMF–water reaction medium (20%, v/v) with an excess of aldehyde. In these conditions, higher product yields and selectivities were achieved operating at a high molar excess of aldehyde by discrete DHAP additions [15].

FucA was almost totally stable at this temperature in the reaction medium, in contrast with significant thermal deactivation at higher temperatures. Moreover, chemical DHAP degradation can be neglected at 4 °C. In consequence, only the desired synthetic aldol addition and the non-desired secondary enzymatic degradation of DHAP will be considered:

(a) Aldol addition

(*S*)-Cbz-alaninal + DHAP

→ (3*R*, 4*R*, 5*S*)-5-(benzyloxycarbonylamino)-5, 6-dideoxy-1-phosphonohex-2-ulose

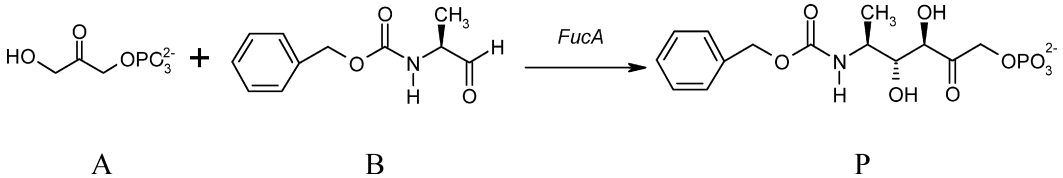

(b) Secondary reaction

DHAP → methylglyoxal + phosphate

3.1.1. Model assumptions

(a) There is experimental evidence that the synthesis reaction (aldol addition) can be treated as apparently irreversible in the reaction medium and conditions indicated above. All the concentration profiles with time led to a final constant product concentration value. If the reverse reaction rate was significant, due to the secondary DHAP consumption, product concentration should decrease, and all DHAP be finally converted to methylglyoxal and phosphate.

(b) The secondary reaction can also be treated as irreversible as the identified products were inorganic phosphate and methylglyoxal which forms a yellow polymer [21], thus driving the reaction to DHAP degradation direction.

(c) A two-substrate ordered mechanism will be postulated for the aldol addition. As it has been previously reported [11], DHAP is forming an enediolate intermediate with the enzyme before the entrance of the acceptor aldehyde. As indicated before, the enediolate intermediate can also led to methylglyoxal and phosphate.

3.2. Rate equations

According to the model assumptions, a mechanism involving two binary complexes, EA (enediolate intermediate) and EP, and a ternary EAB complex, is proposed:

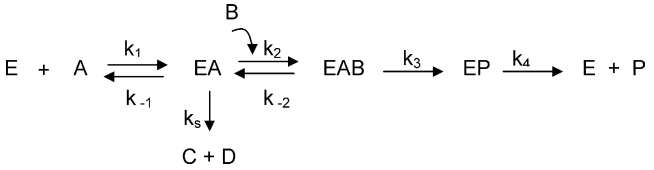

The mass balances can be written as

$$\frac{d[A]}{dt} = -k_s[EA] - k_3[EAB] = -r_s - r \quad (1)$$

$$\frac{d[B]}{dt} = -k_3[EAB] = -r \quad (2)$$

$$\frac{d[P]}{dt} = k_3[EAB] = r \quad (3)$$

$$\frac{d[D]}{dt} = k_s[EA] = r_s \quad (4)$$

$$\frac{d[C]}{dt} = k_s[EA] = r_s \quad (5)$$

where r is the synthesis reaction rate and r_s the secondary reaction rate.

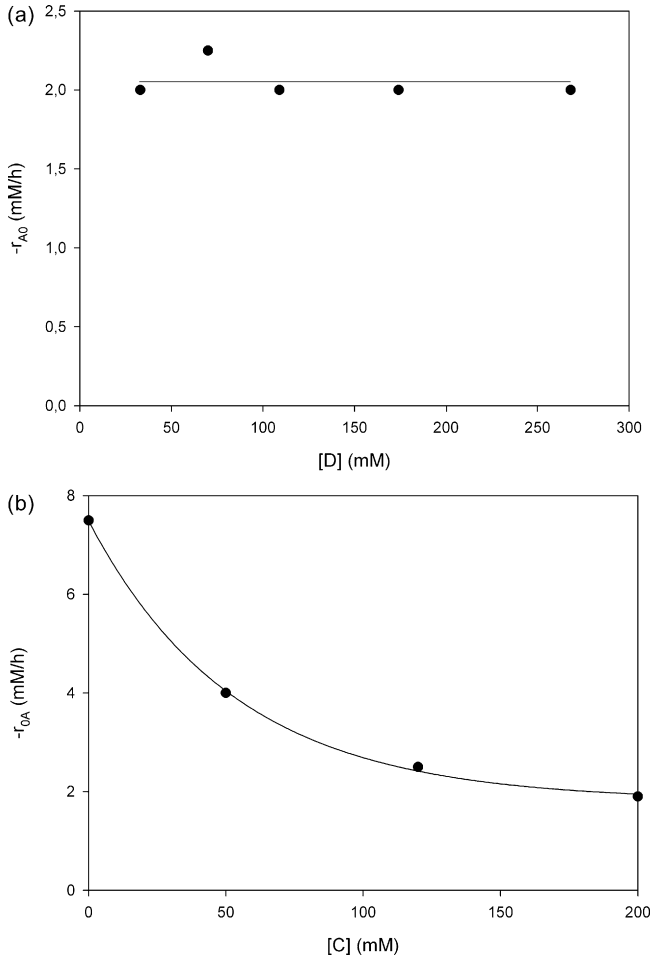

Fig. 1. Initial rate of secondary DHAP conversion in presence of (a) phosphate and (b) methylglyoxal. Experiments performed at an initial DHAP concentration of 40 mM and 3 AU/mL of FucA.

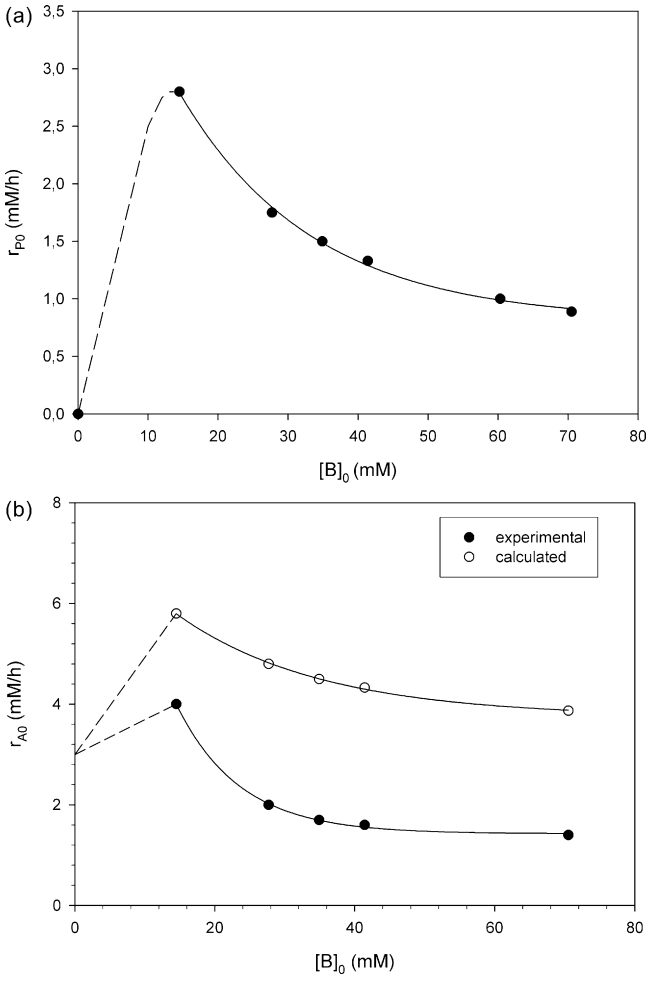

Fig. 2. Reaction rate for aldol additions at different (*S*)-Cbz-alaninal concentrations and 50 mM initial DHAP concentration. (a) Initial rate of product formation. (b) Initial rate of DHAP disappearance. Experimental data (●) and calculated as the addition of product formation rate plus DHAP degradation rate in absence of aldehyde (○).

The rate equations can be obtained by the method proposed by King and Altman [22], as presented in Appendix A.

They are written in the classical form of two-substrate and one-substrate kinetics as

$$r = \frac{r_m[A]\cdot[B]}{K_M K_B + K_B[A] + K_A[B] + [A]\cdot[B]} \quad (6)$$

$$r_s = \frac{r_{ms}[A]}{K_M + [A]} \quad (7)$$

where

$$K_{A'} = \frac{k_{-1}}{k_1}, \qquad K_{A''} = \frac{k_s}{k_1}, \qquad K_B = \frac{k_4(k_{-2}+k_3)}{k_2(k_3+k_4)},$$

$$K_A = \frac{k_3 k_4}{k_1(k_3+k_4)}$$

The Michaelis constant $K_M = K_{A'} + K_{A''}$ is the same for both reactions (as they proceed via the same intermediate EA). The maximum rate is written for each reaction as

$$r_m = \frac{k_3 k_4}{k_3+k_4}[E]_0 \quad \text{and} \quad r_{ms} = k_s[E]_0$$

The above equations are derived without taking into account the possible inhibitory effects of the products and substrates in both reaction rates. They have to be experimentally determined.

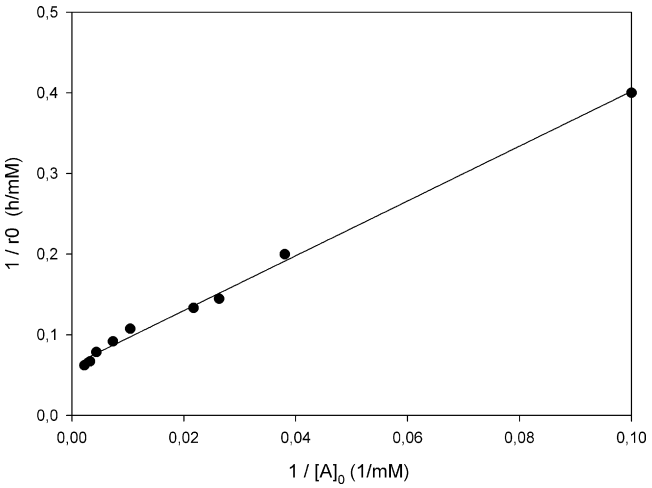

Fig. 3. Lineweaver–Burk plot of secondary reaction initial rate vs. DHAP initial concentration.

3.3. Inhibitory effects

The possible inhibitory effect of the secondary reaction products (methylglyoxal and phosphate) has been previously reported [23]. The experimental elucidation of their influence has been tested in the enzymatic degradation of DHAP (in absence of acceptor aldehyde). It seems reasonable to assume that there will be the same influence in both reactions because they proceed through the same intermediate. The initial rate of DHAP disappearance vs. initial potential inhibitor concentration is presented in Fig. 1. The results are demonstrating that inhibition by methylglyoxal has to be included in the proposed kinetic model, but there is no significant inhibitory effect of inorganic phosphate.

Concerning the substrates, DHAP presented a non-inhibitory behavior (data not shown), whereas (*S*)-Cbz-alaninal has a strong effect as inhibitor. Aldehyde inhibition for other aldolases has been described in literature [24]. Fig. 2a shows the data about (*S*)-Cbz-alaninal influence on product formation initial rate. It becomes clear that the aldehyde is inhibitor of the synthesis reaction even at low concentrations. As pointed before, a molar excess of this substrate is required in order to drive the reaction system towards synthesis, and a less inhibitory low concentration would be favoring the non-desired secondary reaction.

For the same experimental runs, Fig. 2b shows the data of initial DHAP reaction rate and estimated values calculated as the addition of product formation rate plus DHAP degradation rate (in absence of aldehyde). If there was not (*S*)-Cbz-alaninal inhibition on the secondary reaction, both set of data should coincide. As can be seen in Fig. 2, the estimated values are higher, indicating that (*S*)-Cbz-alaninal is also inhibitory on the secondary reaction.

Finally, any possible inhibitory aminopolyol product behavior was not considered because all the preliminary model simulations including product inhibition were not able to describe the experimental product profiles.

3.4. Determination of kinetic parameters

3.4.1. Secondary reaction

A series of experiments of enzymatic degradation of DHAP (in absence of acceptor aldehyde) at DHAP initial concentration between 25 and 450 mM and the same aldolase concentration (3 AU/mL), have been employed for the determination of the secondary reaction kinetic parameters.

K_M and r_{ms} can be determined from experimental data of initial reaction rate, because there is no effect of product inhibition. Fig. 3 shows the Lineweaver–Burk plot and the obtained values

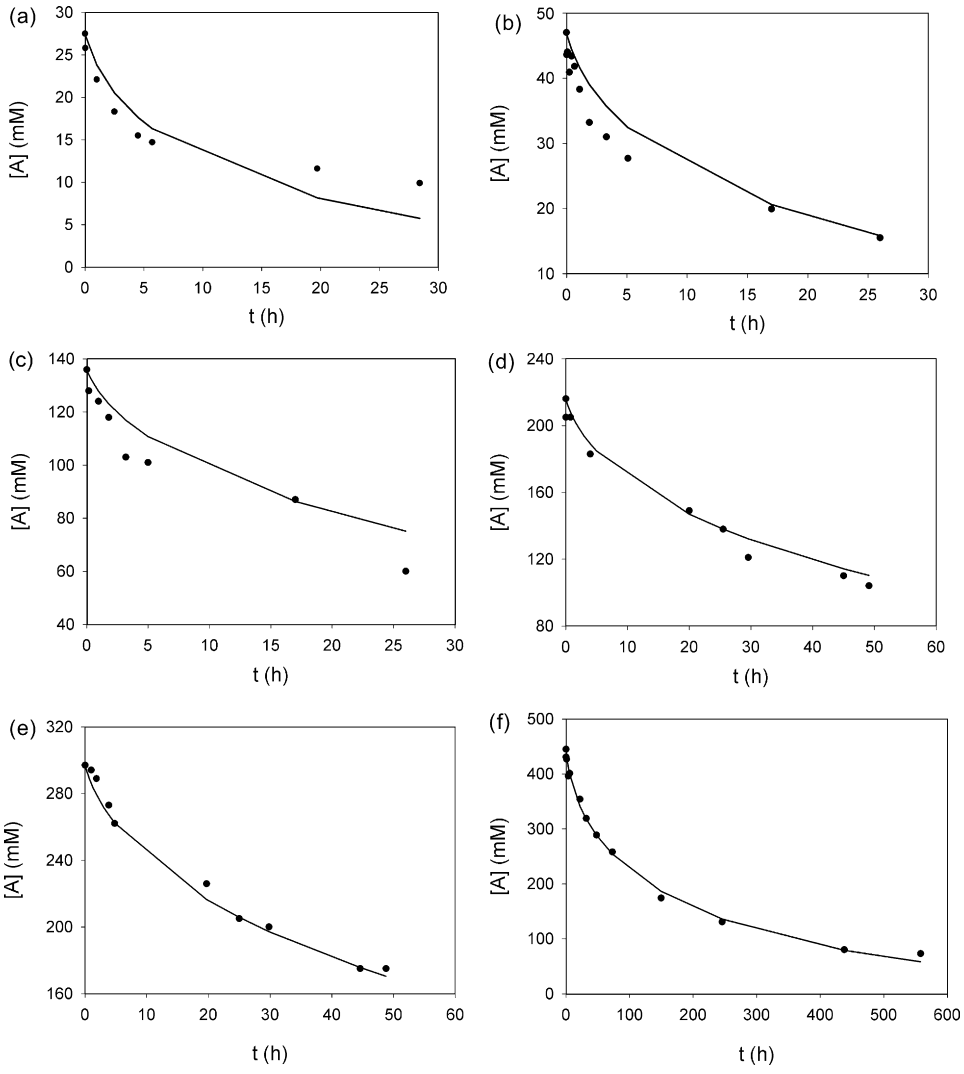

Fig. 4. Experimental data (●) and model predicted (continuous line) DHAP concentration evolution with time for secondary reaction. Initial DHAP concentration (mM): (a) 27.5, (b) 47.0, (c) 136, (d) 216, (e) 297, and (f) 445.

were K_M = 54.7 mM and r_{ms} = 16.1 mM/h, respectively. In order to know the k_{cat} of the secondary reaction, the initial enzyme concentration ($[E]_0$) has been calculated as initial active site concentration. As FucA is a tetramer with four active sites (MW = 24,000 Da per monomer), $[E]_0$ has been calculated as 0.013 mM for 3 AU/mL, giving a $k_{cats} = k_s = 1288\ h^{-1}$.

Using the same experimental series, the data of time evolution of DHAP concentration (presented in Fig. 4), have been employed for the discrimination of methylglyoxal type of inhibition and inhibition constant determination. The different inhibition rate equations (Table 1) have been fitted to experimental data, using the gPROMS software as detailed in Section 2. Employing the above calculated K_M and r_{ms} values, the inhibition constant value which minimizes the objective function was determined. The best fit to the experimental data was obtained for competitive inhibition by methylglyoxal with a value of $k_{iC} = 0.30\ mM^{-1}$.

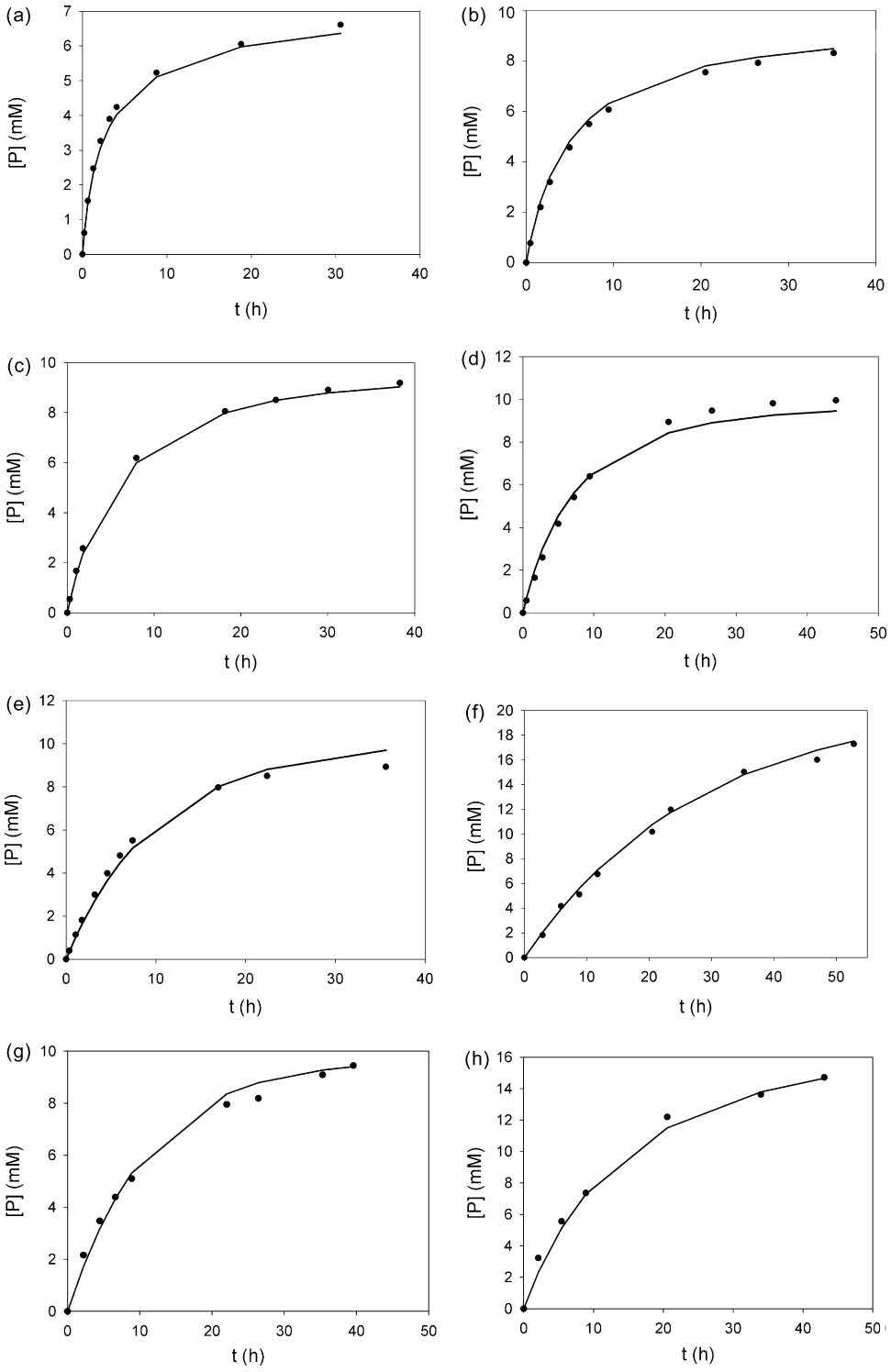

Fig. 5. Experimental data (●) and model predicted (continuous line) product concentration evolution with time for aldol addition reaction. Initial substrates concentration according to Table 1.

Table 1
Inhibition models assayed for the secondary reaction

Inhibition type	
Competitive	$r_s = \frac{r_{ms}[A]}{(K_m \cdot (1+k_{iC}[C])+[A])}$
Non-competitive	$r_s = \frac{r_{ms}[A]}{(K_m+[A]) \cdot (1+k_{iC}[C])}$
Anticompetitive	$r_s = \frac{r_{ms}[A]}{(K_m+[A] \cdot (1+k_{iC}[C]))}$

Table 2
Initial substrates concentration for aldol additions in DMF/water

Experiment	a	b	c	d	e	f	g	h
[DHAP] (mM)	12	12	12	12	12	25.5	11.2	22
[(*S*)-Cbz-alaninal] (mM)	14.5	27.7	34.9	41.4	60.3	92.9	70.5	52.8

With the above results, the rate equation for the secondary reaction can be written as

$$r_s\,(\mathrm{mM/h}) = \frac{1288 \cdot [E]_0[A]}{(54.7 \cdot (1 + 0.30[C] + [A]))} \quad (8)$$

Fig. 4 shows the model predicted DHAP concentration time evolution and the experimental data. There is a reasonable agreement, with a mean deviation of 6.6%. The model fitting is better for high substrate concentration, when experimental measurements can be more accurate and the pseudostationary state hypothesis is more appropriate.

3.4.2. Synthesis reaction

The kinetic parameters of the synthesis reaction have been determined by numerical fitting to experimental data of synthesis employing the same initial enzymatic concentration $[E]_0 = 0.013$ mM (3 AU/mL). The reactions have been performed at different initial DHAP concentrations and different levels of aldehyde excess (see Table 2), in a range corresponding to the solubility of (*S*)-Cbz-alaninal in the reaction medium. The secondary reaction parameters have been set to the values determined above. As an initial guess, the methylglyoxal inhibition constant was set to the same value for the synthesis reaction as in the secondary one. Nevertheless, the best fit to the experimental data was obtained when a different constant value was considered, taking into account the possible differential inhibitory effect on the intermediates involved in the synthesis (EAB and EP). As there is also evidence of (*S*)-Cbz-alaninal inhibition, its inhibition pattern on both reaction rates has to be elucidated. From the different possible models assayed, presented in Table 3, the best fitting to experimental data was obtained for the model including non-competitive inhibition of (*S*)-Cbz-alaninal and competitive inhibition by methylglyoxal on both reactions. The values of the fitted kinetic parameters are $r_m = 20.4$ mM/h, correspond-

Table 3
Kinetic models assayed for the aldol addition

Synthesis reaction rate equation	Secondary reaction rate equation
C competitive inhibition B competitive inhibition $r = \frac{r_m[A] \cdot [B]}{(K_M K_B (1+k_{iC'})(1+k_{iB})+K_B[A](1+k_{iB})+K_A[B]+[A] \cdot [B])}$	C competitive inhibition B competitive inhibition $r_s = \frac{r_{ms}[A]}{K_M(1+k_{iC})(1+k_{iB}B)+[A]}$
C competitive inhibition B anticompetitive inhibition $r = \frac{r_m[A] \cdot [B]}{(K_M K_B (1+k_{iC'})+K_B[A](1+k_{iB})+K_A[B]+[A] \cdot [B](1+k_{iB}))}$	C competitive inhibition B anticompetitive inhibition $r_s = \frac{r_{ms}[A]}{K_M(1+k_{iC})+[A] \cdot (1+k_{iB}B)}$
C competitive inhibition B non-competitive inhibition $r = \frac{r_m[A] \cdot [B]}{(K_M K_B (1+k_{iC'})+K_B[A]+K_A[B]+[A] \cdot [B])(1+k_{iB})}$	C competitive inhibition B non-competitive inhibition $r_s = \frac{r_{ms}[A]}{(K_M(1+k_{iC})+[A]) \cdot (1+k_{iB}B)}$

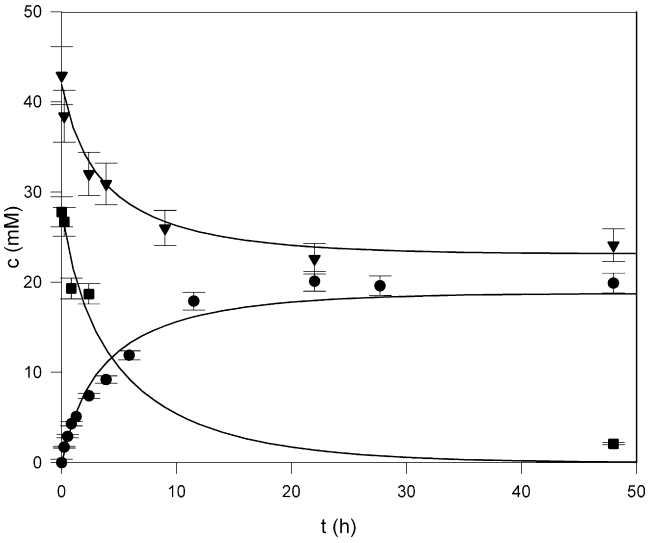

Fig. 6. Concentration profiles for a model validation synthesis catalyzed by 12 AU/mL of enzyme. $[DHAP]_0 = 27.8$ mM and $[(S)\text{-Cbz-alaninal}]_0 = 42.9$ mM. Experimental data: (■) DHAP, (▼) (*S*)-Cbz-alaninal, (●) product. Continuous line: model predicted concentration evolution with time.

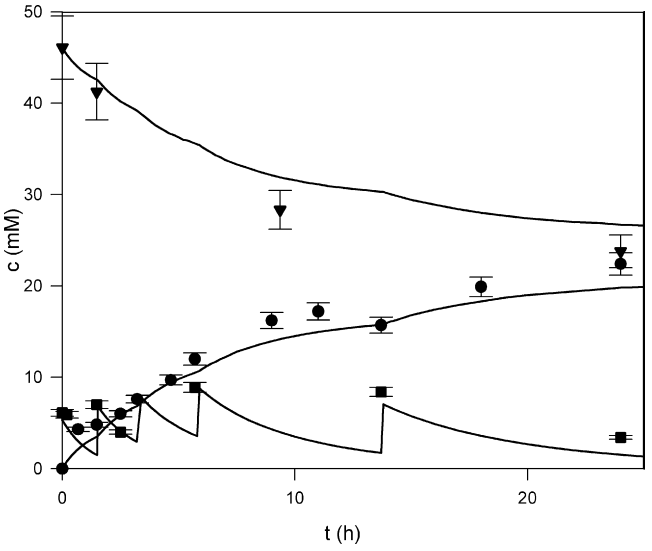

Fig. 7. Concentration profiles for a model validation synthesis with discrete DHAP additions, catalyzed by 12 AU/mL of enzyme. Experimental data: (■) DHAP, (▼) (*S*)-Cbz-alaninal, (●) product. Continuous line: model predicted concentration evolution with time.

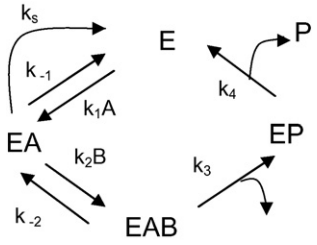

Scheme 1. Cyclic form of mechanism involving all the enzymatic species.

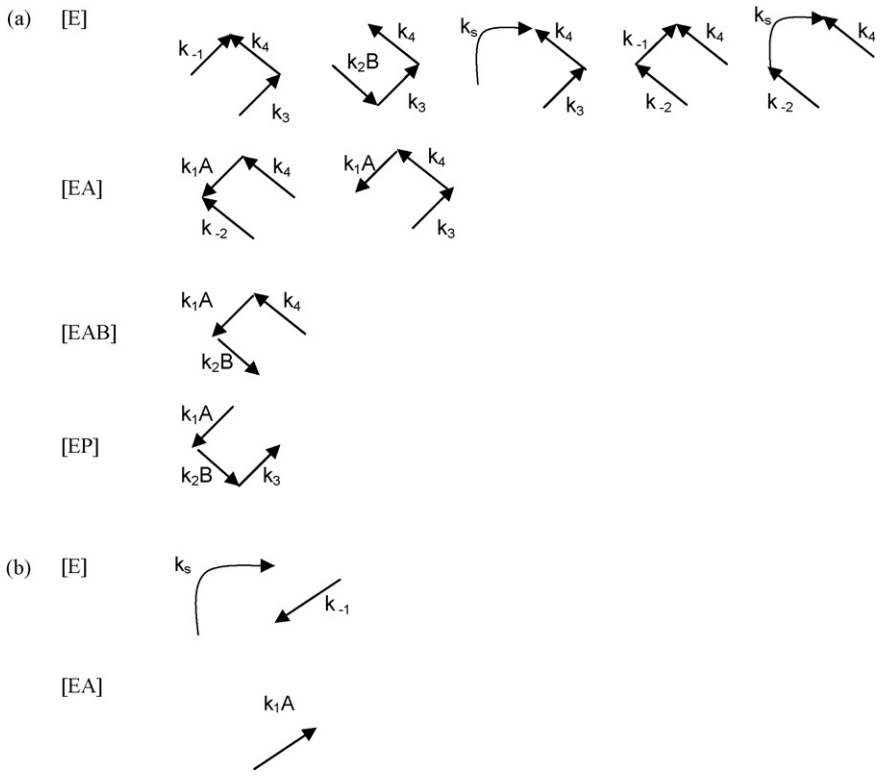

Scheme 2. Patterns of the enzymatic species in the aldol addition reaction (a) and the secondary reaction (b).

ing to a $k_{cat} = 1632\,h^{-1}$ for the synthesis reaction; $K_A = 2.56$ mM; $K_B = 0.262$ mM; $k_{iB} = 0.257$ mM; $k_{iC} = 35.8$ mM.

The final kinetic equations are the following:

$$r\,(\mathrm{mM/h}) = \frac{1632 \cdot [\mathrm{E}]_0[\mathrm{A}] \cdot [\mathrm{B}]}{(14.3 \cdot (1 + 35.8 \cdot [\mathrm{C}]) + 0.262 \cdot [\mathrm{A}] + 2.56 \cdot [\mathrm{B}] + [\mathrm{A}] \cdot [\mathrm{B}])(1 + 0.257 \cdot [\mathrm{B}])} \quad (9)$$

$$r_s\,(\mathrm{mM/h}) = \frac{1288 \cdot [\mathrm{E}]_0[\mathrm{A}]}{(54.7 \cdot (1 + 0.30[\mathrm{C}]) + [\mathrm{A}])(1 + 0.257 \cdot [\mathrm{B}])} \quad (10)$$

The agreement between the experimental and the model calculated product profiles is presented in Fig. 5. The proposed model accurately reproduces the product evolution with time for all the experiments in the range of concentrations considered. The mean deviation was calculated to be 5%.

3.5. Model validation

The kinetic model has been validated employing two experiments at different enzymatic concentration than the calibration ones. Fig. 6 shows the experimental and model predicted time profiles for a synthesis catalyzed by 12 AU/mL of enzyme, and starting from 27.8 mM DHAP and 43 mM aldehyde. Under this conditions, a 74% product yield and a selectivity of 82% was achieved. The model follows fairly well the product and substrates concentration evolution.

As the enhancement of selectivity in favor to the desired reaction can be accomplished by maintaining a high aldehyde excess in the reactor, a fed-batch operation with discrete additions of DHAP would be an appropriate strategy. This operation mode has been implemented by employing the same initial (*S*)-Cbz-alaninal concentration as in the former batch reaction, and distributing the total DHAP amount into five additions. In the mathematical model, each pulse addition is treated as a batch with an initial DHAP concentration equal to the added substrate plus the remaining DHAP in the reactor.

The experimental and model profiles are presented in Fig. 7. As expected, the product yield increased until 88% and the selectivity was 91%. The model predicts properly the concentrations evolution with time, being an appropriate tool for process simulation.

4. Conclusions

A kinetic model describing the aldolase-catalyzed reaction between DHAP and (*S*)-Cbz-alaninal has been developed. The model is taken into account the aldol addition as well as enzymatic DHAP degradation via the same enediolate intermediate. Non-competitive inhibition by (*S*)-Cbz-alaninal and competitive inhibition by methylglyoxal has been identified on both reactions. The kinetic parameters have been determined by numerical fitting to experimental data, and the obtained model has been validated in batch and fed-batch reactions. The mathematical model is able to reproduce fairly well the experimental behavior and, in consequence, can be used in simulation experiments. On the other hand, the model assumptions for this particular aldol addition could be properly extended to other syntheses catalyzed by class II DHAP-dependent aldolases.

Acknowledgements

This work was supported by the Spanish Programme on R&D, Project number CTQ2005-01706/PPQ and by DURSI 2005SGR 00698 Generalitat de Catalunya.

The Department of Chemical Engineering of the UAB constitutes the Biochemical Engineering Unit of the Reference Network in Biotechnology of the Generalitat de Catalunya (XRB).

Appendix A. Deduction of rate equations by King and Altman method

The mechanism has to be written in cyclic form for the four enzymatic species (the three complexes and E), as indicated in Scheme 1.

From the mechanism, the patterns for each of the enzymatic species are presented in Scheme 2 for the case of the aldol addition reaction (2a) and for the secondary reaction alone (2b):

Taking into account that the concentrations of all the enzymatic species are proportional to the summation of the combinations shown in Scheme 2, the derived rate equations were

$$r = \frac{\frac{k_3k_4}{k_3+k_4}[A]\cdot[B]\cdot[E]_0}{\frac{k_{-1}}{k_1}\left[\frac{k_4(k_{-2}+k_3)}{k_2(k_3+k_4)}\right] + \frac{k_s}{k_1}\left[\frac{k_4(k_{-2}+k_3)}{k_2(k_3+k_4)}\right] + \frac{k_4(k_{-2}+k_3)}{k_2(k_3+k_4)}[A] + \frac{k_3k_4}{k_1(k_3+k_4)}[B] + [A]\cdot[B]}$$

$$r_s = \frac{k_s[E]_0\cdot[A]}{((k_{-1}+k_s)/k_1)+[A]}$$

References

[1] C.J. Hamilton, Enzymes in preparative mono- and oligo-saccharide synthesis, Nat. Prod. Rep. 21 (2004) 365–385.
[2] W.D. Fessner, V. Helaine, Biocatalytic synthesis of hydroxylated natural products using aldolases and related enzymes, Curr. Opin. Biotechnol. 12 (2001) 574–586.
[3] T.D. Machajewski, C.H. Wong, The catalytic asymmetric aldol reaction, Angew. Chem. Int. Ed. 39 (2000) 1353–1374.
[4] M. Wymer, E.J. Toone, Enzyme-catalyzed synthesis of carbohydrates, Curr. Opin. Chem. Biol. 4 (2000) 110–119.
[5] A.K. Samland, G.A. Sprenger, Microbial aldolases as C–C bonding enzymes-unknown treasures and new developments, Appl. Microbiol. Biotechnol. 71 (2006) 253–264.
[6] J. Sukuraman, U. Hanefeld, Enantioselective C–C bond synthesis catalyzed by enzymes, Chem. Soc. Rev. 34 (2005) 530–542.
[7] R. Schoevaart, F. van Rantwijk, R.A. Sheldon, Stereochemistry of nonnatural aldol reactions catalyzed by DHAP aldolases, Biotechnol. Bioeng. 70 (2000) 349–352.
[8] W.D. Fessner, G. Sinerius, A. Schneider, M. Dreyer, G.G. Schulz, J. Badia, J. Aguilar, Diastereoselective enzymatic aldol additions: L-rhamnulose and L-fuculose-1-phosphate aldolases from *E. coli*, Angew. Chem. Int. Ed. 30 (1991) 555–558.
[9] O. Eyrisch, M. Keller, W.D. Fessner, Higher-carbon sugars by enzymatic chain extension. Oxidative generation of aldol precursors in situ, Tetrahedron Lett. 35 (1994) 9013–9016.
[10] A.C. Joerger, C. Gosse, W.D. Fessner, G.E. Schulz, Catalytic action of fuculose-1-phosphate aldolase (class II) as derived from structure-directed mutagenesis, Biochemistry 39 (2000) 6033–6041.
[11] M.K. Dreyer, G.E. Schulz, Catalytic mechanism of the metal-dependent fuculose aldolase from *Escherichia coli* as derived from the structure, J. Mol. Biol. 259 (1996) 458–466.
[12] K.M. Koeller, C.H. Wong, Complex carbohydrate synthesis tools for glycobiologists: enzyme-based approach and programmable one-pot strategies, Glycobiology 10 (2000) 1157–1169.
[13] M.H. Fechter, A.E. Stutz, A. Tauss, Chemical and chemo-enzymatic approaches to unnatural ketoses and glycosidase inhibitors with basic nitrogen in the sugar ring, Curr. Org. Chem. 3 (1999) 269–285.
[14] L. Espelt, T. Parella, J. Bujons, C. Solans, J. Joglar, A. Delgado, P. Clapés, Stereoselective aldol additions catalyzed by dihydroxyacetone phosphate dependent aldolases in emulsion systems: preparation and structural characterization of linear and cyclic aminopolyols from aminoaldehydes, Chem. Eur. J. 9 (2003) 4887–4899.
[15] T. Suau, G. Álvaro, M.D. Benaiges, J. López-Santín, Influence of secondary reactions on the synthetic efficiency of DHAP-aldolases, Biotechnol. Bioeng. 93 (2006) 48–55.
[16] L. Espelt, J. Bujons, T. Parella, J. Calveras, J. Joglar, A. Delgado, P. Clapes, Aldol additions of dihydroxyacetone phosphate to N-protected aminoaldehydes catalyzed by L-fuculose-1-phosphate aldolase in emulsion systems: inversion of stereoselectivity as a function of the acceptor aldehyde, Chem. Eur. J. 11 (2005) 1392–1401.
[17] M. Frigerio, M. Santagostino, S. Sputore, A user-friendly entry to 2-iodoxybenzoic acid (IBX), J. Org. Chem. 64 (1999) 4537–4538.
[18] W. Fessner, A. Schneider, O. Eyrisch, G. Sinerius, J. Badia, 6-Deoxy-L-lyxo- and 6-deoxy-L-arabino-hexulose 1-phosphates. Enzymic synthesis by antagonistic metabolic pathways, Tetrahedron Asymm. 41 (1993) 781–790.
[19] B. Zagalak, P. Frey, G.L. Karabatsos, R. Abeles, The stereo-chemistry of the conversion of D and L, 1, 2-propanediols to propionaldehyde, J. Biol. Chem. 241 (1996) 3028–3035.
[20] O. Durany, C. de Mas, J. López-Santín, Fed-batch production of recombinant fuculose-1-phosphate aldolase in *E. coli*, Process Biochem. 40 (2005) 707–716.
[21] J.P. Richard, Acid–base catalysis for the elimination and isomerization reactions of triose phosphates, J. Am. Chem. Soc. 106 (1984) 4926–4936.
[22] E.L. King, C. Altman, A schematic method of deriving the rate laws for enzyme-catalyzed reaction, J. Phys. Chem. 60 (1956) 1375–1378.
[23] W.D. Fessner, C. Walter, Enzymatic C–C bond formation in asymmetric synthesis, Top. Curr. Chem. 184 (1996) 97–194.
[24] R. Schoevaart, F. van Rantwijk, R.A. Sheldon, Facile enzymatic aldol reactions with dihydroxyacetone in the presence of arsenate, J. Org. Chem. 66 (2001) 4559–4562.